

TITLE

ASP Conference Series, Vol. **VOLUME***, **YEAR OF PUBLICATION**

NAMES OF EDITORS

Preliminary Observational Results of Tidal Synchronization in Detached Solar-Type Binary Stars

Søren Meibom

University of Wisconsin - Madison, Wisconsin, USA

Abstract. We present preliminary observational results on tidal synchronization in detached solar-type binary stars in the open clusters M35 (NGC2168; ~ 150 Myr) and M34 (NGC1039; ~ 250 Myr). M35 and M34 provide populations of close late-type binaries with ages that make them attractive observational tests of models of tidal synchronization during the early main-sequence phase. A combined dataset of stellar rotation periods from time-series photometry and binary orbital periods and eccentricities from time-series spectroscopy enables us to determine the angular rotation velocity of the primary star and the orbital angular velocity at periastron. Comparison of the stellar and orbital angular velocities provides information about the level of synchronization in individual binary stars.

1. Introduction

The evolution of stellar angular momentum remains a challenge to our understanding of star formation and early stellar evolution. Angular momentum in solar-type stars is not conserved at any time from birth until death. Long-standing research has demonstrated angular momentum loss via winds, and recently the roles of proto-stellar disks and jets have come to the fore. However, few studies have confronted the role of binary companions, despite the fact that most stars form and evolve in binary systems (Larson 2002; Duquennoy & Mayor 1991).

Tidal forces in close detached binary stars drive the exchange of angular momentum between the stars and their orbital motion (Witte & Savonije 2002; Zahn 1989, 1977; Hut 1981). Depending on the strength of the tidal interactions the stars in a binary system will synchronize their rotation with the orbital motion. The rate of synchronization depends sensitively on the separation of the two stars and on the mechanism for dissipation of kinetic energy into heat within the stars. Understanding the process of tidal dissipation will allow important information about a binary's past angular momentum evolution to be derived, and possibly constrain the conditions of its formation.

The amount of observational data suitable for testing the rate of tidal synchronization in late-type close binaries is sparse. Most of the observational work on synchronization in close binaries has concentrated on early-type stars with radiative envelopes where the mechanism for tidal dissipation is different (Claret & Cunha 1997; Giuricin, Mardirossian, & Mezzetti 1984).

Efforts to theoretically model the evolution of tidal synchronization in late-type stars are ongoing. The main difference between current models lies in the mechanism by which kinetic energy is being dissipated within the stars (the tidal dissipation mechanism). The equilibrium tide theory describes the retardation of the hydrostatic tidal bulge (the equilibrium tide) due to the coupling of the tidal flow to the motion of turbulent eddies in the stellar convective envelope (Zahn 1989; 1977; Hut 1981). The dynamical tide theory describes the excitation, damping and resonances of gravity (g) waves in the radiative zones of stars due to the tidal forcing by the companion star (Savonije & Papaloizou 1983; Zahn 1977). Given an energy dissipation model, tidal theory makes explicit predictions for the evolution of stellar angular momentum in a binary system.

In Figure 1 Zahn & Bouchet (1989; hereinafter ZB) use the equilibrium tide theory to predict the rotational evolution of a solar-mass pair with an initial orbital period of 5 days and an initial orbital eccentricity of 0.3 (dashed curve). Synchronization is rapidly achieved near the stellar birth-line, maintained until shortly after 1 Myr, then lost as the contractions of the stars reduce the tidal forces and spin up the stars. These super-synchronous stars do not regain synchronization until 10^9 yr. Similar modeling predicts pseudo-synchronization with the periastron angular velocity in longer-period eccentric orbits (cf. Hut 1981).

Figure 2 shows the prediction by Witte & Savonije (2002; hereinafter WS) of the rotational evolution of a solar-mass pair with an initial orbital period of 16 days and an initial orbital eccentricity of 0.6. WS applies the dynamical tide theory with inclusion of resonance locking. The stars' initial rotational speed are 20% of their breakup speed, corresponding to a period of 12 hours. Strong retrograde torques rapidly spin down the stars during the first few tens of millions of years ($t \sim 0.08$ Gyr), after which there is a reduction in the stellar spin-down rate lasting to $t \sim 0.5$ Gyr. At that time stellar rotation is approximately synchronous to the orbital angular velocity at periastron. Spin-up to $\sim 1.4 \omega_{per}$ occurs from $t \sim 0.5$ - 0.9 Gyr due to prograde forcing torques, at which point a decrease in stellar separation triggers efficient retrograde forcing of the stars resulting in efficient spin-down to sub-synchronous rotation at $t \sim 3$ Gyr. As the binary orbit circularizes the retrograde forcing diminishes and the stars approach synchronous rotation over the remainder of the main-sequence phase.

Note that the model by ZB includes the pre main-sequence (PMS) evolutionary phase, whereas the WS modeling starts at the ZAMS (Zero Age Main-Sequence). The success of either of these theoretical models can be measured by their ability to predict the observed rotational evolution of stars in close binaries with known ages.

2. Observational Program and Goal

Claret & Cunha (1997) analyzed the validity of Zahn's theories of tidal synchronization using the data from Andersen (1991). This paper is so far the only published study found by us to include late-type stars. Therefore, there is a need for large coeval samples of late-type binaries with accurate information

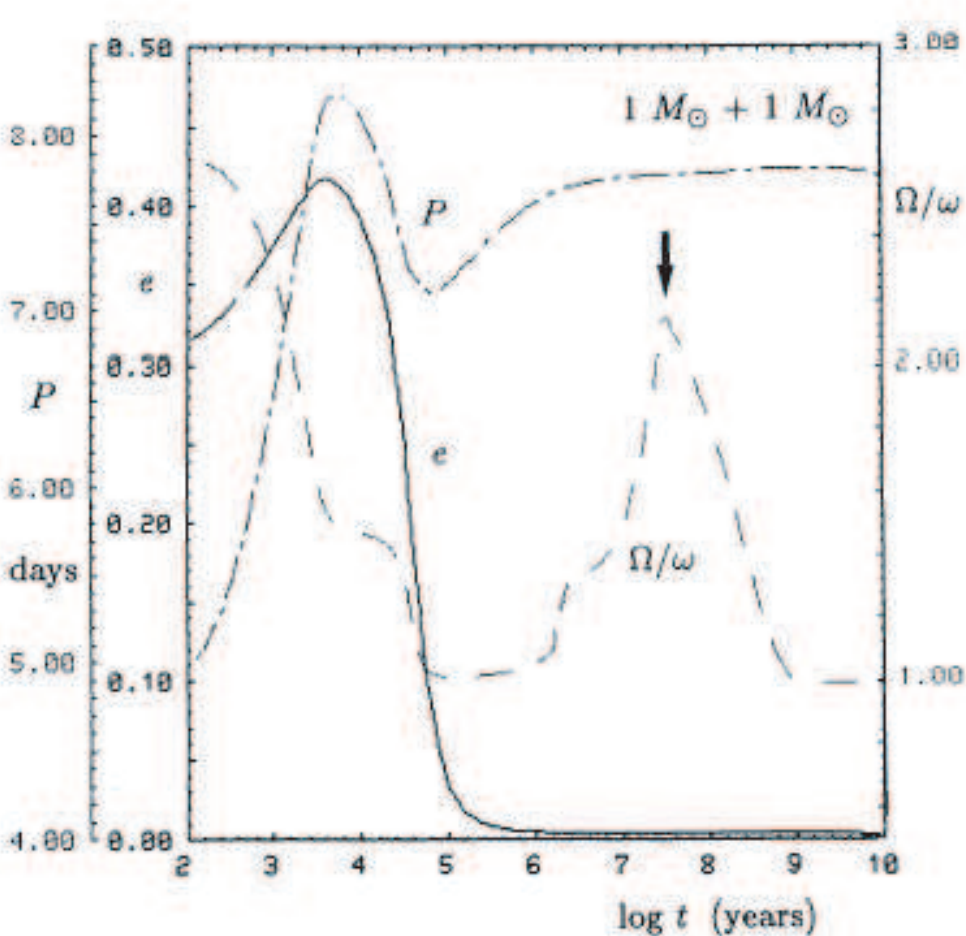


Figure 1. Evolution in time of the ratio between the rotational and orbital velocities (Ω/ω ; dashed curve) for a binary with solar-mass components, an initial orbital period of 5 days, and an initial orbital eccentricity of 0.3 (Zahn & Bouchet 1989).

about the orbital angular velocity as well as the rotational angular velocity of the primary star.

The combination of observed stellar rotation periods and orbital periods and eccentricities for binaries of known ages will directly test the theoretical predictions, and thereby the energy dissipation rates in stellar interiors. Inspired by the success of the distribution of orbital eccentricities versus orbital periods (the $e - \log(P)$ diagram) to constrain theories of tidal circularization (see Mathieu this volume, Meibom & Mathieu 2004, and references therein), we intend to start populating a similar diagram, the $\Omega/\omega - \log(P)$ diagram, with the purpose of constraining theories of tidal synchronization. The $\Omega/\omega - \log(P)$ diagram

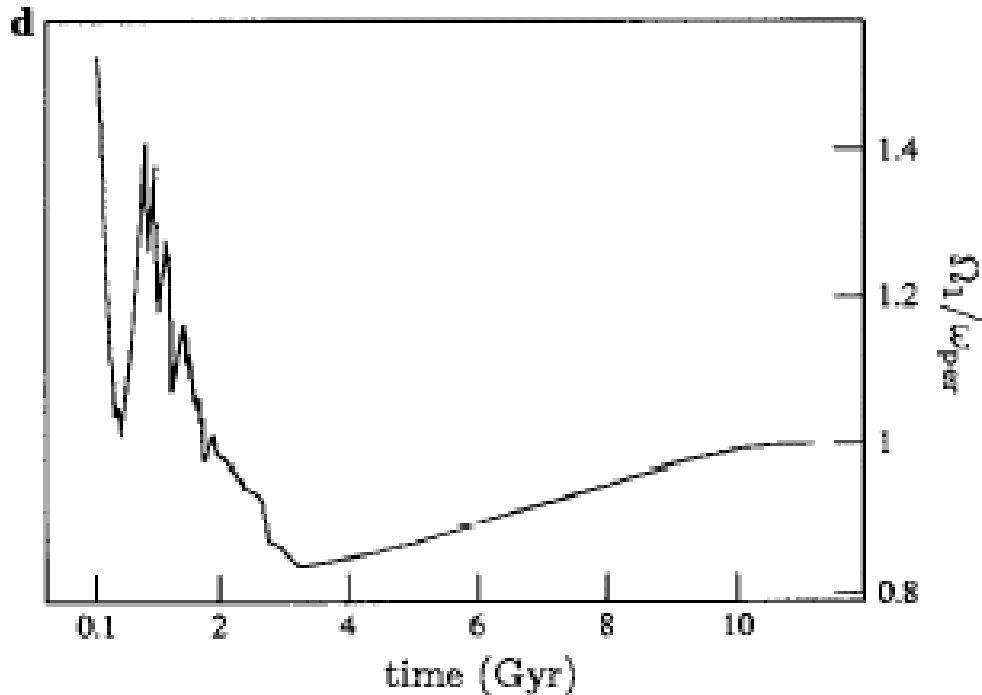


Figure 2. The predicted rotational evolution of the solar-mass components in a close binary with an initial orbital period of 16 days and an initial orbital eccentricity of 0.6 (Witte & Savonije 2002). The stellar angular rotational velocity (Ω_1) is shown relative to the orbital angular velocity at periastron (ω_{per}). The modeling starts at the ZAMS.

represents, as a function of binary period, the ratio of stellar angular velocity of a binary's primary star (Ω) to the orbital angular velocity at periastron (ω).

To obtain that observational goal we have conducted two parallel observational programs on the open clusters M35 (NGC2168; ~ 150 Myr) and M34 (NGC1039; ~ 250 Myr): **1)** High precision radial-velocity surveys to identify binaries and determine their orbital parameters. The surveys are carried out using the WIYN 3.5m telescope, Kitt Peak, Arizona, equipped with the Hydra Multi Object Spectrograph. The surveys are part of the WIYN Open Cluster Study (WOCS) radial-velocity survey program (Mathieu 2000). Radial velocities with measurement accuracies of < 0.5 km/s are achieved to $V = 17$ in 2-hour integrations for late-type stars with narrow lines. The selected brightness range in the two clusters ($12 < V < 17$) correspond to stellar masses from ~ 1.5 to ~ 0.5 solar masses. At the present time, orbital parameters have been determined for 32 spectroscopic binaries in M35 and 18 in M34. **2)** Comprehensive photometric time-series surveys to determine stellar rotation periods from light modulation by starspots on the surfaces of late-type stars. The time-series surveys are based on synoptic data with a frequency of one observation per night from October 2003 till March 2004, and on 2 weeks of 5-6 observations per night in December

2003. The photometric data presented for M35 have been obtained using the WIYN 0.9m telescope at Kitt Peak, Arizona. We have not yet determined rotation periods for stars in M34 but present here results from a similar study by Barnes (private comm.) using the Hall 42-inch telescope at Lowell Observatory, Arizona.

3. Preliminary Results

To populate the $\Omega/\omega - \log(P)$ diagram we are dependent on being able to determine the rotation period of the primary star in binaries for which we also have information about the orbital period and eccentricity. We show in Figure 3 through 6 the preliminary observational results for 4 such binary systems in M35. Relevant orbital and rotational parameters are listed in the figure captions.

Binary 6821 (Figure 3): This single-lined spectroscopic binary (SB1) member of M35 has a circular orbit with a 2.25-day period. We estimate the mass of the primary component to be $0.8 M_{\odot}$ based on a fit of the Yale (Y2) stellar evolutionary models (Yi et al. 2003) to the cluster sequence. The orbital parameters and solution are shown on the left in Figure 3. From the photometric data we found that the integrated stellar brightness of binary 6821 varied with a period of 2.3 days. The phased photometric light-curve is shown on the right in Figure 3, together with the resulting power-spectrum and the unphased light-curve. The similarity of the orbital period and the period of variability in the photometric data suggest that the rotation of the primary star in binary 6821 is synchronized to the orbital motion. The derived ratio of stellar angular velocity to the orbital angular velocity (Ω/ω) is 0.94.

Binary 774 (Figure 4): This SB1 has a circular orbit with a period of 10.3 days. The estimated mass of the primary component is $0.95 M_{\odot}$. The orbital parameters and solution are shown on the left in Figure 4. The photometric data show 10.1-day periodic variability in the integrated stellar brightness of binary 774. The phased photometric light-curve is shown on the right in Figure 4 together with the resulting power-spectrum and the unphased light-curve. Again, the similarity of the orbital period and the period of variability in the photometric data suggest that the rotation of the primary star in binary 774 is synchronized to the orbital motion. The derived ratio of stellar angular velocity to the orbital angular velocity (Ω/ω) is 0.99.

Binary 3121 (Figure 5): This SB1 has an eccentric orbit ($e = 0.27$) with a period of 30.1 days. The estimated mass of the primary component is $0.95 M_{\odot}$. The photometric data show a 2.8-day periodic variability in the integrated stellar brightness of the binary. The phased photometric light-curve is shown on the right in Figure 5. The period of variability in the photometric data thus suggest that the rotation of the primary star in binary 3121 is super-synchronous. The ratio of stellar angular velocity to the orbital angular velocity at periastron (Ω/ω) is 5.83.

Binary 701 (Figure 6): This SB1 has a highly eccentric orbit ($e = 0.54$) with a period of 8.2 days. The estimated mass of the primary component is $0.77 M_{\odot}$. The photometric data show a 3.6 day periodic variability in the integrated stellar brightness of the binary. The phased photometric light-curve is shown on the right in Figure 6. Comparing the orbital period and the period of variability

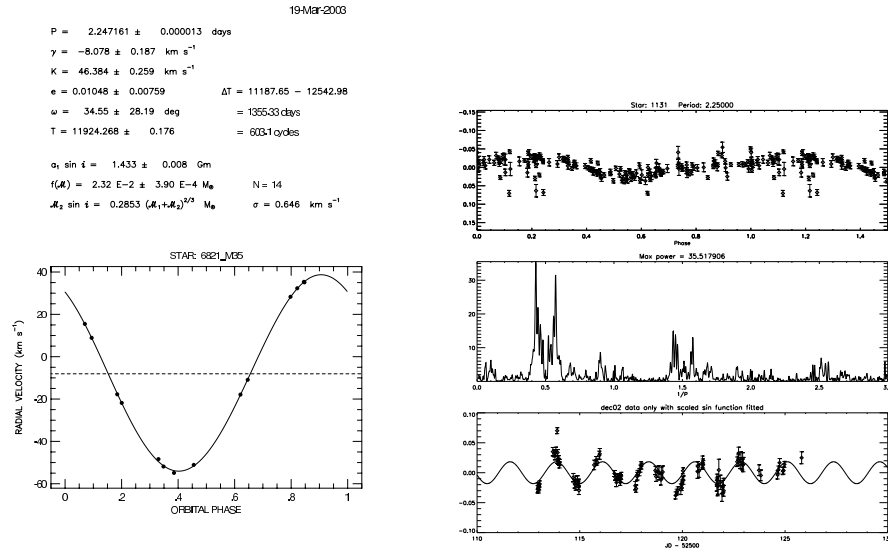


Figure 3. **Left:** The orbital parameters and phased radial- velocity curve for binary 6821. The best fit orbit has an eccentricity of 0.01 and a period of 2.25 days. **Right:** The photometric light-curve for binary 6821 phased to a period of 2.3 days together with the power spectrum in frequency space and the unphased light-curve. A sine curve with a period of 2.3 days has been overplotted on the unphased photometric data.

in the photometric data might suggest that the primary star is rotating with super-synchronous velocity. However, due to the high eccentricity the orbital velocity at periastron is high and the derived ratio of stellar angular velocity to the orbital angular velocity at periastron (Ω/ω) is 0.37. The primary in binary 701 is thus rotating at a sub-synchronous velocity.

4. The $\Omega/\omega - \log(P)$ Diagram

We show in Figure 7 the $\Omega/\omega - \log(P)$ diagram with all preliminary observational results from M35 and M34. A value of 1 for the ratio of rotational to orbital angular velocity ($\Omega/\omega = 1$) implies synchronization or pseudo- synchronization, whereas a value above or below 1 indicates super- or sub-synchronous stellar rotation, respectively. Black circles represent binary stars in M35 for which we have secure determination of the orbital period and eccentricity, and the rotational period of the primary star. Grey circles represent binaries in M35 for which we are not 100% confident in the values for the orbital period and/or eccentricity. The black open square represents a binary in M34. All binary stars shown in Figure 7 are cluster members.

The results presented here are preliminary and the number of binary stars with secure observational determination of orbital and stellar angular velocities is small. Further populating the $\Omega/\omega - \log(P)$ diagram may enable us to

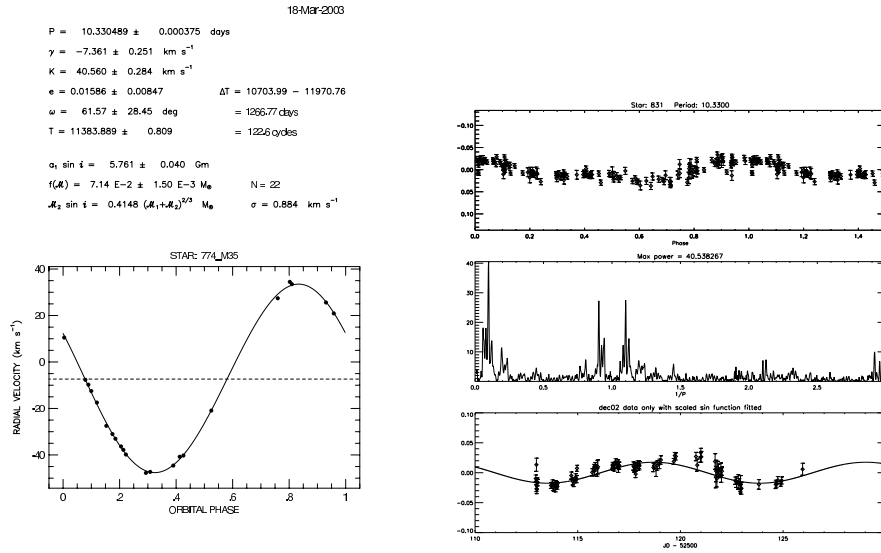


Figure 4. **Left:** The orbital parameters and phased radial velocity curve for binary 774. The best fit orbit has an eccentricity of 0.01 and a period of 10.3 days. **Right:** The photometric light-curve for binary 774 phased to a period of 10.1 days together with the power spectrum in frequency space and the unphased light-curve. A sine curve with a period of 10.1 days has been overplotted the unphased photometric data.

determine a *synchronization period* at the age of the binary population. The synchronization period will be defined as the orbital period at which binaries at the age of the population goes from being synchronized or pseudo-synchronized to being non-synchronized. The synchronization period will play an important role in constraining the efficiency and evolution of synchronization predicted by the theories of tidal synchronization, much as the *circularization period* is constraining the theories of tidal circularization (Meibom & Mathieu 2004; Mathieu this volume).

Despite the small number of binary systems currently available, some interesting individual systems offer constraints on current theoretical models. Figure 8 show the $\Omega/\omega - \log(P)$ diagram for binaries with periods shortward of 100 days. The coeval binaries 774 and 701 in M35 offer an intriguing challenge to the theoretical models. Binary 774 has been synchronized and circularized at a period of 10.3 days while binary 701 at a shorter period of 8.2 days has not been either pseudo-synchronized or circularized. In addition, a single binary from M34 is shown with an orbital period of 4.4 days (black open square). The rotational period of the primary star is measured at 8 days (Barnes, priv. comm.). The binary orbit is circular and thus the primary star is rotating sub-synchronously ($\Omega/\omega = 0.48$). This is a particularly interesting result because the timescale for tidal synchronization is thought to be shorter than the timescale of tidal circularization (Zahn 1977; Hut 1981).

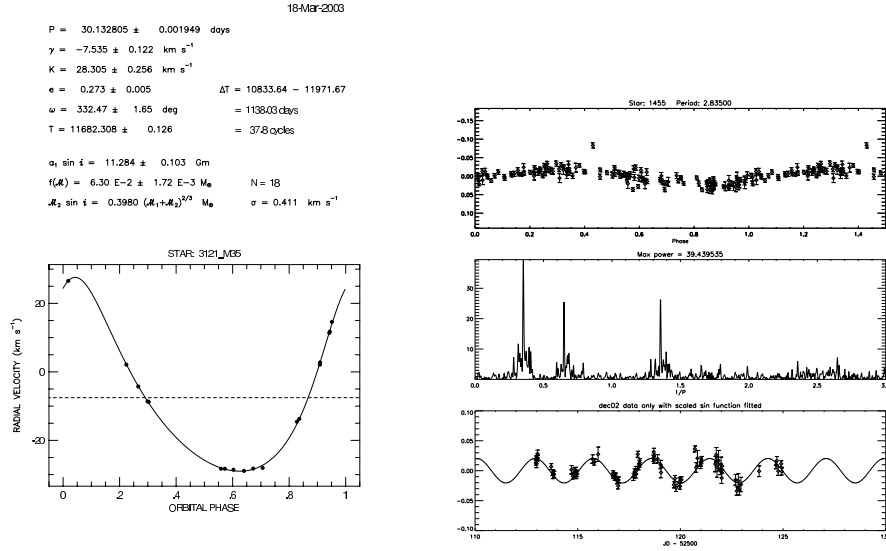


Figure 5. **Left:** The orbital parameters and phased radial velocity curve for binary 3121. The best fit orbit has an eccentricity of 0.01 and a period of 30.1 days. **Right:** The photometric light-curve for binary 3121 phased to a period of 2.8 days together with the power spectrum in frequency space and the unphased light-curve. A sine curve with a period of 2.8 days has been overplotted the unphased photometric data.

Acknowledgments S.M. thanks his dissertation advisor Robert D. Mathieu. We are thankful to the University of Wisconsin - Madison Astronomy Department, to NOAO, and to the WIYN Telescope Director George Jacoby for the time granted on the WIYN telescopes. We thank the WIYN Observatory staff for exceptional and friendly support. We would like to express our appreciation for the help from Keivan Stassun and Sydney Barnes in planning the photometric time-series surveys, and to Keivan Stassun for the help with the process of deriving stellar rotation periods. We thank the organizers for an exciting and well organized meeting in the wonderful city of Granada. This work has been supported by NSF grant AST 97-31302 and by a Ph.D fellowship from the Danish Research Agency (Forskningstyrelsen) to S.M.

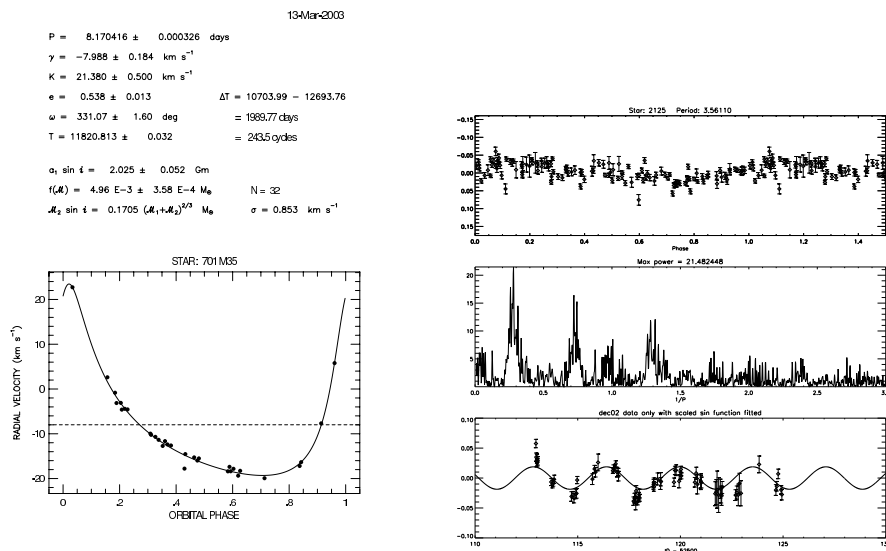


Figure 6. **Left:** The orbital parameters and phased radial velocity curve for binary 701. The best fit orbit has an eccentricity of 0.54 and a period of 8.2 days. **Right:** The photometric light-curve for binary 701 phased to a period of 3.6 days together with the power spectrum in frequency space and the unphased light-curve. A sine curve with a period of 3.6 days has been overplotted the unphased photometric data.

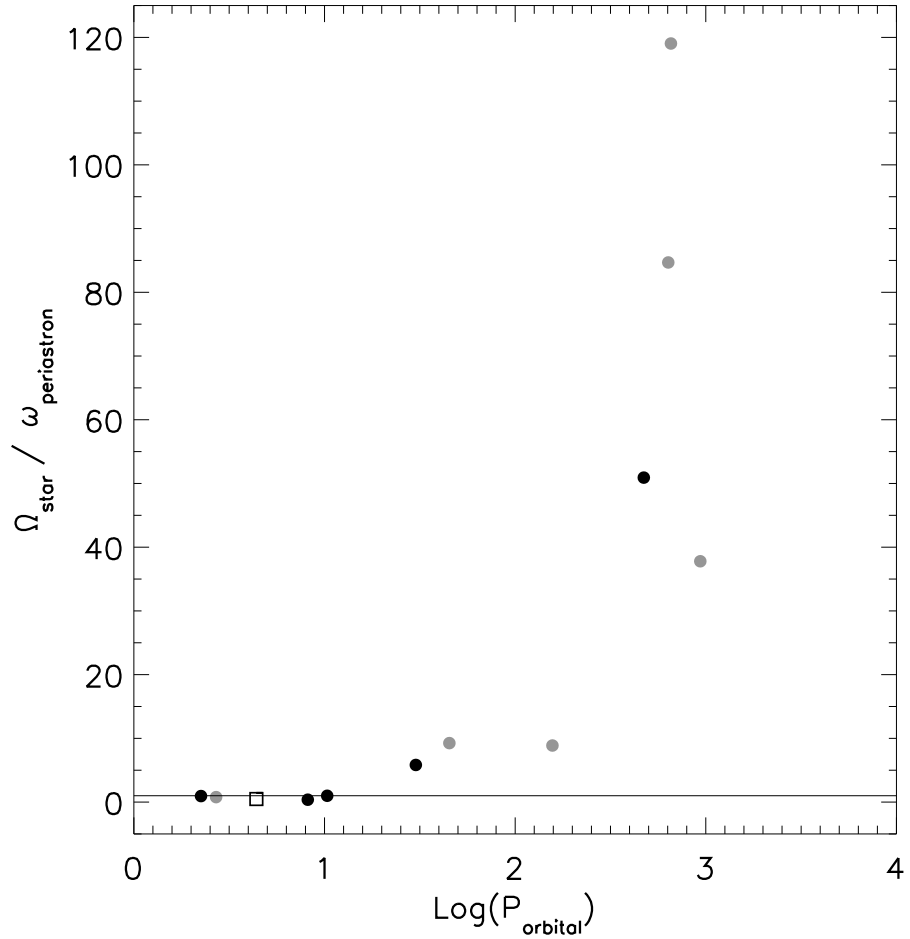


Figure 7. The ratio of angular rotational velocity of the primary star (Ω) to the orbital angular velocity at periastron (ω) for close detached binary stars in M35 and M34. Black circles represent binary stars in M35 for which we have secure determination of the orbital period and eccentricity, and the rotational period of the primary star. Grey circles represent binaries in M35 for which we are not 100% confident in the values for the orbital period and/or eccentricity. The black open square represents a binary star in M34.

References

Barnes, S. 2004, in prep.
 Andersen, J. 1991, A&A Rev., 3, 91
 Claret, A., & Cunha, N. C. S. 1997, A&A, 318, 187

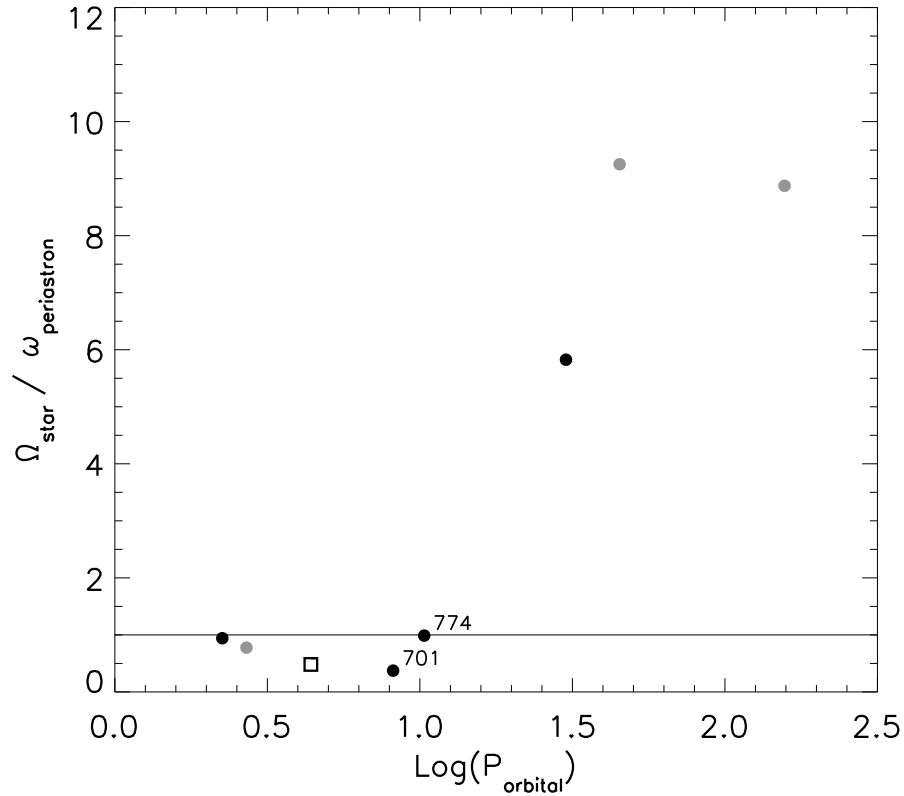


Figure 8. The $\Omega/\omega - \log(P)$ diagram with focus on binaries with orbital periods shortward of 100 days. All symbols are the same as in Figure 7.

Duquennoy, A., & Mayor, M. 1991, A&A, 248, 485
 Giuricin, G., Mardirossian, F., & Mezzetti, M. 1984, A&A, 134, 365
 Hut, P. 1981, A&A, 99, 126
 Larson, R. B. 2002, MNRAS, 332, 156
 Mathieu, R. D. 2000, ASP Conf. Ser. 198, 517
 Meibom, S., & Mathieu, R. D. 2004, ApJ, in press
 Savonije, G. J., & Papaloizou, J. C. B. 1983, MNRAS, 203, 581
 Witte, M., & Savonije, G. J. 2002, A&A, 386, 222
 Yi, S. K., Kim, Y., & Demarque, P. 2003, ApJS, 144, 259
 Zahn, J.-P. 1977, A&A, 57, 383

Zahn, J.-P. 1989, A&A, 220, 112

Zahn, J.-P., & Bouchet, L. 1989, A&A, 223, 112